RSC Advances

PAPER

View Article Online
View Journal | View Issue

Cite this: *RSC Adv.*, 2025, **15**, 39864

Probing the hydrogen bonding of guest functional groups with [2.2.2]-cryptand/KF host *vs.* with solvent by ^{19}F-NMR spectroscopy

So Yeon Lee,†[a] Young-Ho Oh, †[b] Han Bin Oh *[a] and Sungyul Lee *[b]

We present a method for probing the local environment surrounding ammonium, hydroxyl, and carboxyl functional groups in solution by analyzing the ^{19}F-NMR chemical shifts of [2.2.2]-cryptand ([2.2.2])/KF/protonated amino acid (AAH^+) complexes. Specifically, we examine two competing structural features-solvation of guest functional groups *versus* complexation with the host-by monitoring hydrogen bonding interactions in deuterated ethylene glycol (EG-d_6) and deuterated acetonitrile (CD_3CN). Model systems including [2.2.2]/KF/$NH_4^+Cl^-$, [2.2.2]/KF/choline$^+Cl^-$ ([2.2.2]/KF/Ch^+Cl^-), and 24-crown-8/CsF/betaine/H^+Cl^- were employed to benchmark the chemical shift signatures associated with specific hydrogen bonding motifs. Based on the observed ^{19}F NMR peaks, we assign the structures of [2.2/2]/AAH^+ (AA = proline (Pro), threonine (Thr)) complexes in each solvent. In EG-d_6, both complexes exhibit [$-NH_3^+\cdots F^-$] hydrogen bonding, while the carboxyl group in $ProH^+$ and the carboxyl and hydroxyl groups in $ThrH^+$ remain solvated and unbound to the host. In contrast, in CD_3CN, the carboxyl group in $ProH^+$ and both the carboxyl and ammonium groups in $ThrH^+$ directly engage in hydrogen bonding with F^-. These findings support the use of ^{19}F-NMR spectroscopy as a sensitive probe of the [2.2.2]/KF/protonated amino acid system in solution and provide insight into potential structural correlations between solution-phase and gas-phase complexes.

Received 8th September 2025
Accepted 14th October 2025

DOI: 10.1039/d5ra06750b

rsc.li/rsc-advances

Introduction

Understanding host–guest interactions[1–6] in solution is of significant interest, both as a foundation for molecular recognition principles[7–9] and self-assembly processes,[10–13] and for the rational design of supramolecular systems such as artificial enzymatic catalysts,[14–17] gene delivery vectors,[18,19] bioimaging agents,[20,21] and stimuli-responsive materials.[22–25] In contrast with the gas phase, where techniques such as electrospray ionization/mass spectrometry combined with infrared multiphoton dissociation (ESI/MS/IRMPD)[26–37] allow probing of host–guest configurations, investigating these interactions in solution remains challenging. Specifically, acquiring detailed structural information on guest biomolecules and deciphering the microenvironment, *i.e.*, host complexation *vs.* solvation, of their functional groups is often difficult using conventional experimental methods such as ^{1}H-NMR spectroscopy, collision-induced dissociation,[38,39] or ion-mobility spectrometry.[40–42] While these techniques can offer valuable insights into some aspects of host–guest behaviours, they often fall short of providing a comprehensive picture.

In this study, we investigate the complexes of $ProH^+$ and $ThrH^+$ with [2.2.2]/KF in solution (CD_3CN and EG-d_6; see Fig. 1), as model systems for macrocyclic host–biomolecule guest interactions. We use ^{19}F-NMR spectroscopy as a sensitive probe of the [2.2.2]/KF/protonated amino acid system in solution, remedying the ineffectiveness (missing or extreme broadening of resonance signals) of ^{1}H-NMR technique for examining H-bonding features of bio/organic functional groups such as carboxyl, hydroxyl and ammonium. The notable sensitivity of the ^{19}F chemical shifts on the H-bonding environment around the metal fluorides as agents for nucleophilic reactions[43] and also as a probe for determining the interactions between the [2.2.2]/KF/choline chloride model system[44] is harnessed here to elucidate the interactions between [2.2.2]/KF and protonated forms of the amino acids proline and threonine. For the [2.2.2]/

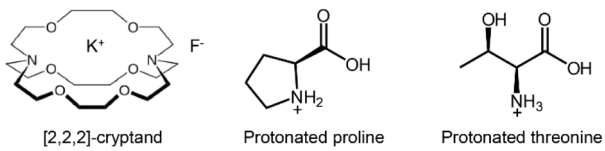

[2,2,2]-cryptand Protonated proline Protonated threonine

Fig. 1 Components of [2.2.2]/KF/$ProH^+$ and [2.2.2]/KF/$ThrH^+$ non-covalent host–guest complexes.

[a]*Department of Chemistry, Sogang University, Seoul 121-742, Republic of Korea. E-mail: hanbinoh@sogang.ac.kr*

[b]*Department of Applied Chemistry, Kyung Hee University, Gyeonggi 17104, Republic of Korea. E-mail: sylee@khu.ac.kr*

† These authors contributed equally to this work: So Yeon Lee and Young-Ho Oh.

KF/ProH$^+$ complex, we examine which of the two functional groups (ammonium or carboxyl) interacts with the host and/or the solvent molecules in EG-d_6 and in CD_3CN. In the case of [2.2.2]/KF/ThrH$^+$, which features three adjacent acidic functional groups (Fig. 1), we explore which combinations (–NH_3^+/–OH, –NH_3^+/–CO_2H, or –NH_3^+/–OH/–CO_2H) engage in hydrogen bonding with the [2.2.2]/KF host.

To interpret the observed ^{19}F-NMR chemical shifts, we leverage the high sensitivity of ^{19}F NMR to H-bonding interactions involving F^-.[43,44] Reference complexes, *i.e.*, [2.2.2]/KF/$NH_4^+Cl^-$, [2.2.2]/KF/Ch$^+Cl^-$, and 24-crown-8/CsF/Betaine/H^+Cl^-, are employed to benchmark the configurations of [2.2.2]/KF/ProH$^+$ and [2.2.2]/KF/ThrH$^+$ in solution. The [2.2.2]-cryptand ([2.2.2]; Fig. 1) was selected as a host component due to its strong affinity for coordinating metal cations. This macrocyclic ligand is well known as a highly effective K^+ chelator, making it useful in applications such as metal ion sensing and phase-transfer catalysis (PTC).[45] When complexed with KF, [2.2.2] can bind K^+ and position F^- as a sensitive probe to detect the local environment of guest molecules bearing acidic functional groups, *e.g.*, –NH_3^+, –OH, and –COOH. The chemical shift of F^- in the ^{19}F NMR spectrum can indicate whether F^- interacts with the ammonium group, carboxylic/hydroxyl groups, or solvent molecules.

We also perform gas-phase structure calculations for the [2.2.2]/KF/AAH$^+$ (AA = Pro, Thr) complexes to provide insight into potential structural correlations between solution-phase and gas-phase complexes. The most thermodynamically stable forms of these complexes correspond to configurations where the carboxyl (and hydroxyl, in the case of ThrH$^+$) are solvated in solution but become 'naked', that is, disengaged from the [2.2.2]/KF host, in the gas phase. We discuss the configurations and relative thermodynamic stabilities (based on Gibbs free energy) of these gas-phase species, focusing on the structural correlation between the solution and gas phases, as bridged by ESI/MS procedures.

Experimental: methods and materials

All chemicals and solvents used in this study were purchased from commercial suppliers and used without further purification. 24-crown-8, cesium fluoride, potassium fluoride, betaine hydrochloride, ammonium chloride, deuterated acetonitrile (CD_3CN), deuterated ethylene glycol (EG-d_6), proline, and threonine were obtained from Sigma Aldrich (St. Louis, MO, USA). For NMR analysis, sample mixtures such as 24-crown-8/CsF/aineH$^+$ and [2.2.2]/CsF/ProH$^+$ were prepared by mixing the components in a 1 : 1 : 1 molar ratio and dissolving them in CD_3OD or EG-d_6. Both ^{1}H and ^{19}F NMR spectra were recorded at 298 K using a JEOL 500 MHz spectrometer (JNM-ECZL500R, JEOL Ltd, Tokyo, Japan). Chemical shifts (δ) are reported in parts per million (ppm), referenced externally to trimethylsilane (TMS; δ 0.0 ppm) for ^{1}H NMR and trifluorotoluene (TFT; δ −63.72 ppm) for ^{19}F NMR.

Computational details

All calculations were performed using the wB97X-D[46] density functional theory (DFT) method. A 6-311G** basis set was applied for all atoms. All computations were carried out using the Gaussian 16 software package.[47] We employed the supramolecule – continuum model, treating the solvent in the first shell around the complex as explicit molecules while others are accounted for as SMD continuum.[48]

Vibrational frequency analyses were conducted to confirm the nature of all stationary points; all minima were verified to have no imaginary frequencies. A scaling factor of 0.927 was applied to the calculated IR frequencies of the free hydroxyl and carboxyl groups to match the experimental reference values (3680 and 3560 cm^{-1}, respectively).[29,49]

Results and discussion

Structures of [2.2.2]/KF/ProH$^+$ and [2.2.2]/KF/ThrH$^+$ non-covalent host–guest complexes in solution (CD_3CN and EG-d_6)

Fig. 2 presents the ^{19}F-NMR spectra and calculated structures for two model systems: [2.2.2]/KF/$NH_4^+Cl^-$ in EG-d_6 and 24-crown-8/CsF/Betaine/H^+Cl^- in CD_3CN. In Fig. 2a, the intense ^{19}F resonance at −137.54 ppm observed for [2.2.2]/KF/$NH_4^+Cl^-$ is readily assigned to a [$F^-\cdots NH_4^+$] hydrogen bond. This chemical shift serves as a diagnostic marker for [$F^-\cdots NH_3^+$]

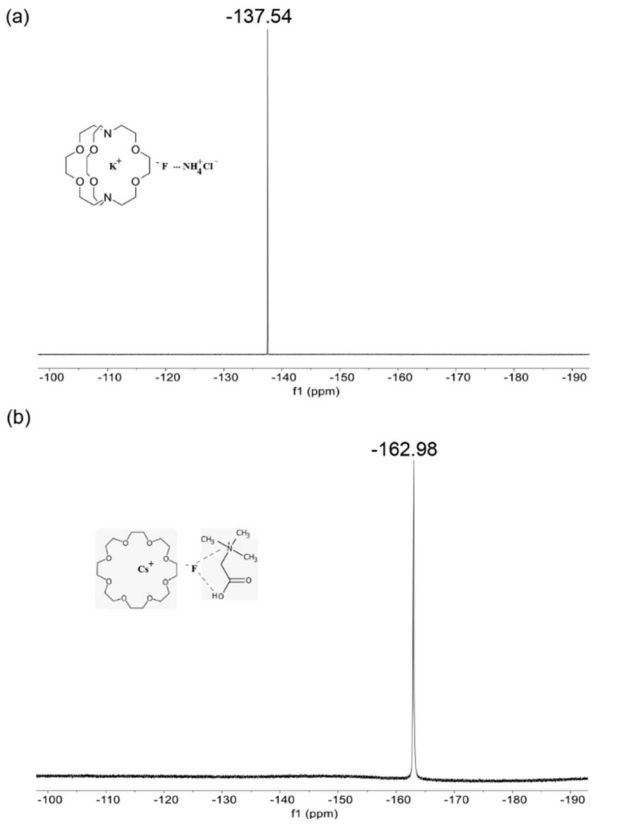

Fig. 2 ^{19}F-NMR spectrum and schematic structure of (a) [2.2.2]/KF/$NH_4^+Cl^-$ in EG-d_6 (b) 24-crwon-8/CsF/BetH^+Cl^- in CD_3CN. Chemical shift in ppm.

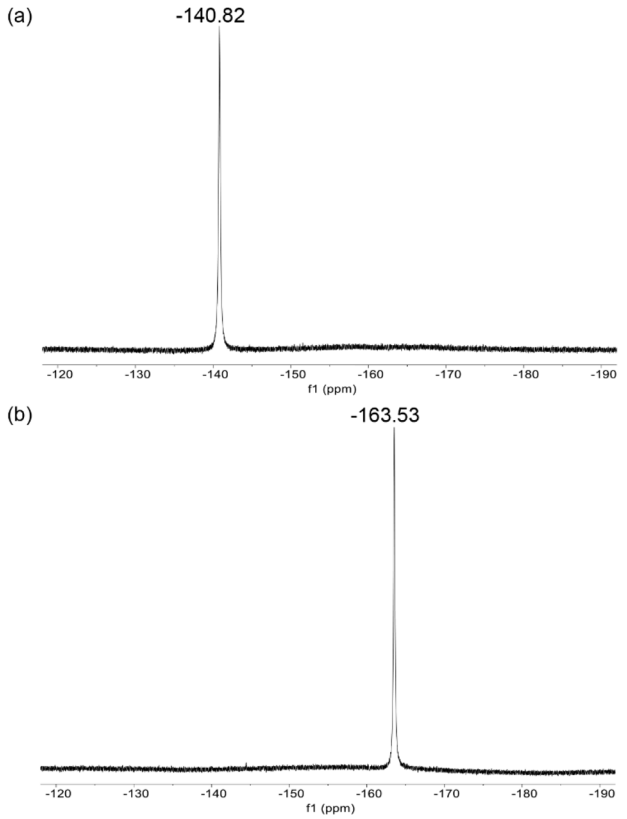

Fig. 3 ^{19}F-NMR spectrum of [2.2.2]/KF/ProH$^+$ (a) in EG-d_6 (b) in CD_3CN. Chemical shift in ppm.

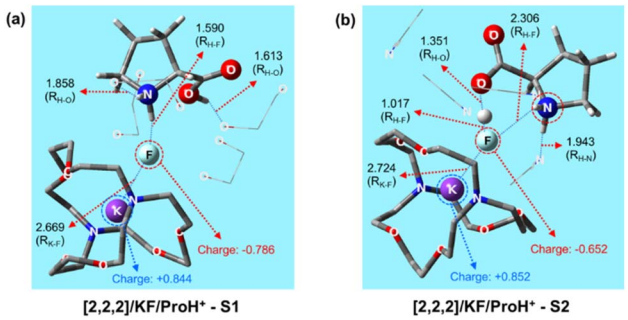

Fig. 4 Calculated lowest Gibbs free energy structure of [2.2.2]/KF/ProH+ (a) in EG-d_6 (b) in CD3CN. Distance in Å. Natural bond orbital charges in *e* unit. Blue background represents the solvent continuum.

interactions in EG-d_6. Fig. 2b shows the ^{19}F-NMR spectrum of 24-crown-8/CsF/Betaine/H$^+$Cl$^-$ in CD_3CN, featuring a prominent signal at −162.98 ppm, characteristic of a [–NH_3^+···F$^-$···HO_2C–] hydrogen bonding motf. Similar downfield shifts are observed for the [2.2/2]/KF/ProH$^+$ and [2.2.2]/KF/ThrH$^+$ complexes in CD_3CN, as discussed below.

Fig. 3 shows the ^{19}F-NMR spectra of the [2.2.2]/KF/ProH$^+$ complex in EG-d_6 and CD_3CN. In EG-d_6, a sharp peak at −140.82 ppm closely matches that of the $NH_4^+Cl^-$ model system (Fig. 2a), suggesting that only the ammonium group binds to the [2.2.2]/KF host, while the carboxyl group remains solvated and excluded from host interaction. In contrast, in CD_3CN, the appearance of a strong peak at −163.53 ppm indicates that both the ammonium and carboxyl groups participate in the [–NH_3^+···F$^-$···HO_2C–] hydrogen bonding with F$^-$, in analogy with the 24-crown-8/CsF/Betaine/H$^+$Cl$^-$ complex (see Fig. 2b; −162.98 ppm).

Quantum chemical calculations[50–53](Fig. 4) support these structural assignments. In EG-d_6, the H···F distance is 1.590 Å, indicating no proton transfer from the ammonium group to F$^-$. Additionally, an EG-d_6 molecule appears to solvate and spatially separate the carboxyl group from the [2.2.2] ring. In CD_3CN, the carboxyl proton seems to be transferred to F$^-$ ($R_{H\cdots F} = 1.017$ Å), while the ammonium group is shielded by solvent molecules, remaining distant from the host. Although K$^+$ is chelated inside the cavity of the cryptand [2.2.2], it still exists as a contact ion-pair, not as a naked ion, as revealed in our previous paper.[43] We may also rule out the possibility of the formation of the complex [2.2.2]/KCl/AAH$^+$F$^-$ in which the solvent-separated F$^-$ (devoid of Coulomb interaction with K$^+$) forms H-bond with the ammonium or carboxyl in AAH$^+$, because the latter complex would give rise to a peat at ∼ −101 ppm (Fig. S10 in SI, ref. 43).

Fig. 5 shows the ^{19}F-NMR spectra of the [2.2.2]/KF/ThrH$^+$Cl$^-$ complex in solution. In EG-d_6, a strong peak at −140.91 ppm closely resembles that of the ProH$^+$ complex (−140.82 ppm), indicating that only the ammonium group binds to the host, while both the hydroxyl and carboxyl groups are solvated and

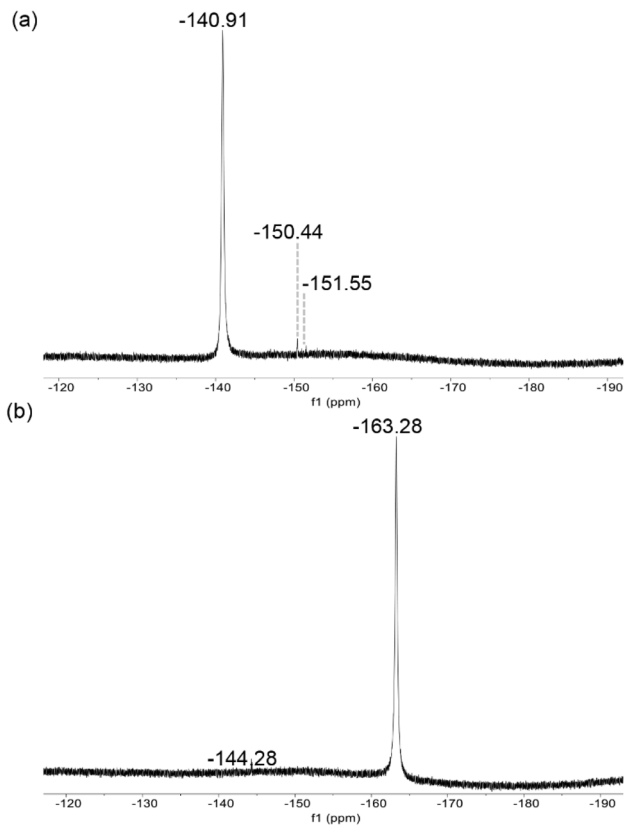

Fig. 5 ^{19}F-NMR spectrum of [2.2.2]/KF/ThrH$^+$Cl$^-$ (a) in EG-d_6 (b) in CD_3CN.

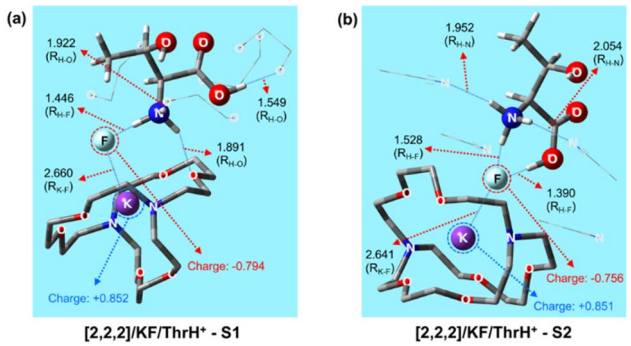

Fig. 6 Calculated lowest Gibbs free energy structure of [2.2.2]/KF/ThrH$^+$ (a) in EG-d_6 (b) in CD3CN. Distance in Å. Blue background represents the solvent continuum.

excluded from interaction with [2.2.2]. In CD_3CN, a peak at −163.28 ppm is observed, comparable to the signals at −162.98 ppm (BetaineH$^+$) and −163.53 ppm (ProH$^+$), suggesting that a [–NH_3^+···F^-···HO_2C–] interaction forms, with the hydroxyl group remaining solvated and unbound to the host. This observation is consistent with the greater acidity of the carboxyl group compared to the hydroxyl, as F^- preferentially forms hydrogen bonds with the more acidic proton. Notably, the absence of a signal near −178 ppm, associated with a fully formed [F^-···HO_2C–] interaction, indicates that proton transfer from the carboxyl to F^- does not occur in this case. This conclusion is further supported by the lack of a peak near −117 ppm (Fig. S1, SI), which would correspond to a [–NH_3^+···F^-···HO–] hydrogen bond as observed in [2.2.2]/KF/Ch^+Cl^- in DMSO-d_6.[44]

These NMR interpretations align well with the calculated lowest Gibbs free energy structures of the [2.2.2]/KF/ThrH$^+$ complex in both solvents. In EG-d_6 (Fig. 6a), a [–NH_3^+···F^-] interaction is observed ($R_{H\cdots F} = 1.446$ Å), along with a possible weak hydrogen bond ($R_{H\cdots F} = 1.891$ Å) between the ammonium and an oxygen atom of the host. In CD_3CN, both the ammonium and carboxyl groups interact with F^- ($R_{H\cdots F} = 1.528$ and 1.390 Å), while the hydroxyl remains fully solvated and excluded from interaction with the [2.2.2] ring. Importantly, neither proton is fully transferred to F^- in this case.

Calculated structures of [2.2.2]/KF/ProH$^+$ and [2.2.2]/KF/ThrH$^+$ non-covalent host–guest complexes in the gas phase

The ESI/MS and IRMPD techniques have proven to be powerful tools for generating and characterizing gas-phase host–guest complexes. One of the most intriguing questions in supramolecular chemistry is whether the structural features of host–guest complexes in solution is preserved upon transfer to the gas phase. Although there is no definitive experimental proof for this proposition, recent observations offer compelling clues. Notably, highly unfavorable gas-phase configurations of permethylated cyclodextrin (perm-CD) complexes with AAH$^+$ (AA = alanine, isoleucine) have been reported.[42,54] Subsequent theoretical studies proposed that these gas-phase conformers originate from the most stable solution-phase configuration[54–58] guesting a structural correlation between the two phases.

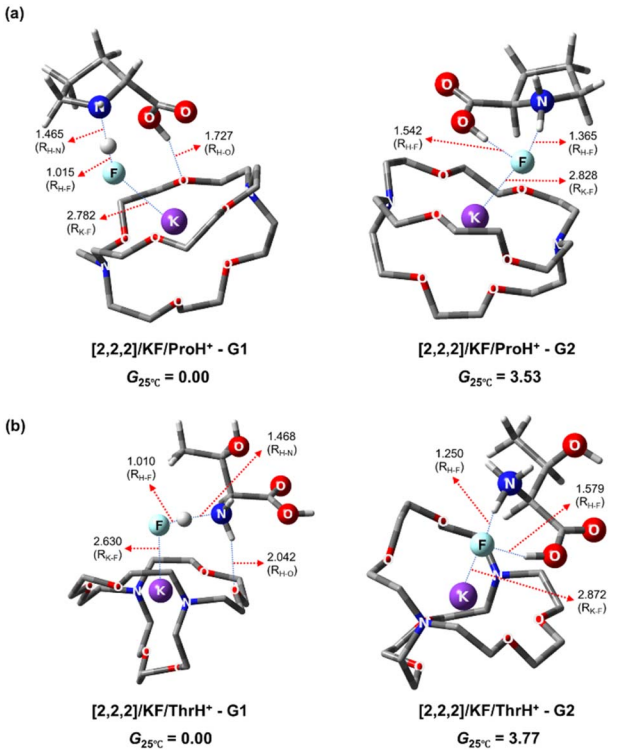

Fig. 7 Calculated structures of (a) [2.2.2]/KF/ProH$^+$ (b) [2.2.2]/KF/ThrH$^+$ complex in the gas phase. Relative Gibbs free energy in kcal mol^{-1}, distance in Å.

To facilitate experimental validation of this hypothesis in the present systems, we performed DFT calculations on the gas-phase structures and IR spectra of [2.2.2]/KF/AAH$^+$ complexes (AA = Pro, Thr). Fig. 7a displays the lowest Gibbs free energy structures of the [2.2.2]/KF/ProH$^+$ complex in the gas phase. In the thermodynamically more favored (Gibbs free energy lower by 3.5 kcal mol^{-1}) configuration, [2.2.2]/KF/ProH$^+$-G1, the ammonium group alone forms a hydrogen bond with F^-, closely resembling the solution-phase structure [2.2.2]/KF/ProH$^+$-S1 (Fig. 4a). This structural similarity suggests a clear correlation between the gas- and solution-phase structures. However, the removal of solvent during the ESI/MS process induces subtle chages: (1) the ammonium proton is transferred to F^- ($R_{H\cdots F} = 1.015$ Å), and (2) the carboxyl group engages in a weak hydrogen bond with the [2.2.2] ring ($R_{H\cdots F} = 1.727$ Å).

In contrast, the second gas-phase structure, [2.2.2]/KF/ProH$^+$-G2, mirrors the solution-phase structure [2.2.2]/KF/ProH$^+$-S2, in which both the ammonium and carboxyl groups form hydrogen bonds with F^-. However, in the gas phase, the H···F bond in G2 is considerably elongated (1.542 Å) compared to the corresponding bond in the solution-phase counterpart (1.017 Å). These two contrasting proton transfer behaviors may underlie the higher thermodynamic stability of G1 over G2 in the gas phase.

Fig. 7b shows the two lowest Gibbs free energy structures of the [2.2.2]/KF/ThrH$^+$ complex in the gas phase. In the more stable conformer [2.2.2]/KF/ThrH$^+$-G1, the ammonium group forms a hydrogen bond with F^-, while a proton is transferred

from the carboxyl group to F^- ($R_{H\cdots F}$ = 1.010 Å), indicating an acid–base reaction. Additionally, the ammonium group forms a weak hydrogen bond with the [2.2.2] ring ($R_{H\cdots O}$ = 2.042 Å). The carboxyl and hydroxyl groups, previously solvated in the solution-phase structure [2.2.2]/KF/ThrH$^+$-S1, are now 'naked' in the gas phase. In the second gas-phase conformer, [2.2.2]/KF/ThrH$^+$-G2 (Gibbs free energy higher by 3.5 kcal mol^{-1} than G1), both the ammonium and carboxyl groups interact with F^-, while the hydroxyl group remains unbound, *i.e.*, 'naked'. Thus, the gas-phase structures [2.2.2]/KF/ThrH$^+$-G1 and [2.2.2]/KF/ThrH$^+$-G2 appear to correspond closely to the solution-phase structures [2.2.2]/KF/ThrH$^+$-S1 and [2.2.2]/KF/ThrH$^+$-S2, respectively, with minor adjustments due to the absence of solvent. Fig. S2 and S3 in SI present the calculated infrared spectra of these two gas-phase complexes to be compared with the experimental IRMPD spectra for structural identification in the gas phase.

A natural question arises: which gas-phase structures of [2.2.2]/KF/AAH$^+$ (AA = Pro, Thr) are most likely to be observed in ESI/MS experiments? If our hypothesis holds – that gas-phase structures reflect the most thermodynamically stable solution-phase configurations-then [2.2.2]/KF/AAH$^+$-S1 is expected to predominate in the gas phase when generated from EG-d_6 solution, while [2.2.2]/KF/AAH$^+$-S2 should be observed when CD_3CN is the solvent. The thermodynamically disadvantageous gas phase complexes, which were observed in our past works, may eventually relax thermodynamically. In the thermal non-equilibrium gas-phase environment produced from the solution phase by the ESI/MS techniques, however, the rearrangement of the H-bonds in the complexes may be difficult, giving rise to 'kinetically trapped' gas-phase host–guest complexes.

The appearance of thermodynamically less favorable gas-phase species originating from the most stable CD_3CN solution structures would thus provide further evidence for what we term a 'thermodynamic reversal'. This concept offers a valuable framework for inferring solution-phase host–guest configurations from their gas-phase counterparts.

Conclusions

We have elucidated the structures of the [2.2.2]/KF/ProH$^+$ and [2.2.2]/KF/ThrH$^+$ host–guest complexes in solution using ^{19}F-NMR spectroscopy. By monitoring the hydrogen bonding behavior of guest functional groups (ammonium, hydroxyl, and carboxyl) with [2.2.2]/KF host *versus* solvent molecules, we identified distinct ^{19}F chemical shifts characteristic of each interaction type. Our results reveal that the local environment surrounding the hydroxyl group is highly dependent on the solvent nature, with significant differences observed between the polar aprotic solvent CD_3CN and the protic solvent EG-d_6. Although the DFT methods employed here for the [2.2.2]/KF/AAH$^+$ complexes seem to predict reasonable solution-phase structures, using more accurate *ab initio* theory and PCM methods would help to validate them rigorously. This will be carried out in our future works.

We also predicted, through gas-phase calculations, that the thermodynamically less favorable complexes featuring 'naked' acidic functional groups, originating from solution-phase structures in CD_3CN, would be detectable in the gas phase. These observations support the validity of using gas-phase structures to infer key features of solution-phase host–guest interactions.

Overall, our findings demonstrate the effectiveness of ^{19}F-NMR spectroscopy as a powerful probe for characterizing the microenvironment of functional groups in small guest molecules. However, for larger hosts (*e.g.*, cyclodextrins, cucurbiturils, calixarenes) and more complex guests (*e.g.*, peptides, proteins), complementary techniques such as ^{1}H-NMR spectroscopy, collision-induced dissociation, and ion-mobility spectrometry may be required to achieve a comprehensive understanding.

We anticipate that this study will stimulate further investigation into host–guest chemistry, particularly in leveraging combined spectroscopic and computational approaches to unravel the subtle interplay of non-covalent interactions in increasingly complex supramolecular systems.

Author contributions

S. L. and H. B. O. supervised the overall project and secured the funding, conceived the idea and designed the study. S. Y. L. carried out ^{19}NMR experiments, and Y.-H. O. did quantum chemical calculations. S. Y. L. and Y.-H. O. acquired and analyzed the data, co-writing the draft. S. L. and H. B. O. co-wrote the final version of the manuscript, to which all authors have given approval.

Conflicts of interest

There are no conflicts to declare.

Data availability

The data supporting this article have been included as part of the supplementary information (SI). Supplementary information is available. See DOI: **https://doi.org/10.1039/d5ra06750b**.

Acknowledgements

This work was supported by grants from the National Research Foundation of Korea funded by the Ministry of Education (2018R1A6A1A03024940, 2021R1A2C2007397), and the KISTI Supercomputing Center. HBO is thankful to the research grant supported by Korea Environmental Industry & Technology Institute (KEITI) through Technology develop project for safety management of household chemical products, funded by Korea Ministry of Climate, Energy and Environment (MCEE) (RS-2025-02223473).

Notes and references

1 D. J. Cram and J. M. Cram, *Science*, 1974, **183**, 803–809.
2 X. Ma and Y. Zhao, *Chem. Rev.*, 2015, **115**, 7794–7839.

3 Q. Da Hu, G. P. Tang and P. K. Chu, *Acc. Chem. Res.*, 2014, **47**, 2017–2025.
4 D. Jiao, J. Geng, X. J. Loh, D. Das, T. Lee and O. A. Scherman, *Angew. Chem., Int. Ed.*, 2012, **51**, 9633–9637.
5 P. Hurtado, F. Gámez, S. Hamad, B. Martínez-Haya, J. D. Steill and J. Oomens, *J. Phys. Chem. A*, 2011, **115**, 7275–7282.
6 J. Lee, S.-S. Lee, S. Lee and H. Bin Oh, *Molecules*, 2020, **25**, 4048.
7 C. Kim, S. S. Agasti, Z. Zhu, L. Isaacs and V. M. Rotello, *Nat. Chem.*, 2010, **2**, 962–966.
8 C. A. Schalley, *Int. J. Mass Spectrom.*, 2000, **194**, 11–39.
9 G. Yu, K. Jie and F. Huang, *Chem. Rev.*, 2015, **115**, 7240–7303.
10 R. F. Service, *Science*, 2005, **309**, 95.
11 V. Percec, A. E. Dulcey, V. S. K. Balagurusamy, Y. Miura, J. Smidrkal, M. Peterca, S. Nummelin, U. Edlund, S. D. Hudson and P. A. Heiney, *Nature*, 2004, **430**, 764–768.
12 H. Zhang, K. T. Nguyen, X. Ma, H. Yan, J. Guo, L. Zhu and Y. Zhao, *Org. Biomol. Chem.*, 2013, **11**, 2070–2074.
13 F. M. Menger, *Proc. Natl. Acad. Sci. U. S. A.*, 2002, **99**, 4818–4822.
14 F. Ortega-Caballero, C. Rousseau, B. Christensen, T. E. Petersen and M. Bols, *J. Am. Chem. Soc.*, 2005, **127**, 3238–3239.
15 R. Villalonga, R. Cao and A. Fragoso, *Chem. Rev.*, 2007, **107**, 3088–3116.
16 L. Zhao, J. Cai, Y. Li, J. Wei and C. Duan, *Nat. Commun.*, 2020, **11**, 1–11.
17 J. Czescik, Y. Lyu, S. Neuberg, P. Scrimin and F. Mancin, *J. Am. Chem. Soc.*, 2020, **142**, 6837–6841.
18 K. Miyata, N. Nishiyama and K. Kataoka, *Chem. Soc. Rev.*, 2012, **41**, 2562–2574.
19 M. E. Davis, J. E. Zuckerman, C. H. J. Choi, D. Seligson, A. Tolcher, C. A. Alabi, Y. Yen, J. D. Heidel and A. Ribas, *Nature*, 2010, **464**, 1067–1070.
20 Y. Wang, H. Gao, J. Yang, M. Fang, D. Ding, B. Z. Tang and Z. Li, *Adv. Mater.*, 2021, **33**, 1–8.
21 C. Liu, H. Yu, Q. Li, C. Zhu and Y. Xia, *ACS Appl. Mater. Interfaces*, 2018, **10**, 16291–16298.
22 J. Zhang, Z.-H. Zhou, L. Li, Y.-L. Luo, F. Xu and Y. Chen, *Mol. Pharm.*, 2020, **17**, 1100–1113.
23 L.-J. Chen and H.-B. Yang, *Acc. Chem. Res.*, 2018, **51**, 2699–2710.
24 D.-H. Qu, Q.-C. Wang, Q.-W. Zhang, X. Ma and H. Tian, *Chem. Rev.*, 2015, **115**, 7543–7588.
25 M. Zhang, X. Yan, F. Huang, Z. Niu and H. W. Gibson, *Acc. Chem. Res.*, 2014, **47**, 1995–2005.
26 P. Kebarle and U. H. Verkerk, *Mass Spectrom. Rev.*, 2009, **28**, 898–917.
27 Z. Takats, J. M. Wiseman, B. Gologan and R. G. Cooks, *Science*, 2004, **306**, 471–473.
28 C. P. McNary, Y. W. Nei, P. Maitre, M. T. Rodgers and P. B. Armentrout, *Phys. Chem. Chem. Phys.*, 2019, **21**, 12625–12639.
29 C. N. Stedwell, J. F. Galindo, K. Gulyuz, A. E. Roitberg and N. C. Polfer, *J. Phys. Chem. A*, 2013, **117**, 1181–1188.
30 N. Geue, *Anal. Chem.*, 2024, **96**, 7332–7341.
31 J. S. Ho, A. Gharbi, B. Schindler, O. Yeni, R. Brédy, L. Legentil, V. Ferrières, L. L. Kiessling and I. Compagnon, *J. Am. Chem. Soc.*, 2021, **143**, 10509–10513.
32 O. Yeni, S. Ollivier, B. Moge, D. Ropartz, H. Rogniaux, L. Legentil, V. Ferrières and I. Compagnon, *J. Am. Chem. Soc.*, 2023, **145**, 15180–15187.
33 H. Yao, J. D. Steill, J. Oomens and R. A. Jockusch, *J. Phys. Chem. A*, 2011, **115**, 9739–9747.
34 R. Cheng, E. Loire and T. D. Fridgen, *Phys. Chem. Chem. Phys.*, 2019, **21**, 11103–11110.
35 J. Seo, W. Hoffmann, S. Warnke, M. T. Bowers, K. Pagel and G. von Helden, *Angew. Chem., Int. Ed.*, 2016, **55**, 14173–14176.
36 D. Scuderi, V. Lepere, G. Piani, A. Bouchet and A. Zehnacker-Rentien, *J. Phys. Chem. Lett.*, 2014, **5**, 56–61.
37 M. Burt, K. Wilson, R. Marta, M. Hasan, W. S. Hopkins and T. McMahon, *Phys. Chem. Chem. Phys.*, 2014, **16**, 24223–24234.
38 G. Carroy, V. Lemaur, J. De Winter, L. Isaacs, E. De Pauw, J. Cornil and P. Gerbaux, *Phys. Chem. Chem. Phys.*, 2016, **18**, 12557–12568.
39 A. J. Arslanian, N. Mismash and D. V Dearden, *J. Am. Soc. Mass Spectrom.*, 2022, **33**, 1626–1635.
40 C. Vicent, V. Martinez-Agramunt, V. Gandhi, C. Larriba-Andaluz, D. G. Gusev and E. Peris, *Angew. Chem., Int. Ed.*, 2021, **133**, 15540–15545.
41 B. A. Link, A. J. Sindt, L. S. Shimizu and T. D. Do, *Phys. Chem. Chem. Phys.*, 2020, **22**, 9290–9300.
42 S.-S. Lee, J. Lee, J. H. Oh, S. Park, Y. Hong, B. K. Min, H. H. L. Lee, H. I. Kim, X. Kong and S. Lee, *Phys. Chem. Chem. Phys.*, 2018, **20**, 30428–30436.
43 J. G. Jeong, Y.-H. Oh, T. H. Park, S.-S. Lee, D. W. Kim and S. Lee, *Nat. Commun.*, 2025, **16**, 1236.
44 S. Y. Lee, Y. H. Oh, H. Bin Oh and S. Lee, *Phys. Chem. Chem. Phys.*, 2025, **27**, 14391–14396.
45 H.-J. Lee and K. Maruoka, *Nat. Rev. Chem.*, 2024, **8**, 851–869.
46 J. Da Chai and M. Head-Gordon, *Phys. Chem. Chem. Phys.*, 2008, **10**, 6615–6620.
47 M. J. Frisch, G. W. Trucks, H. B. Schlegel, G. E. Scuseria, M. A. Robb, J. R. Cheeseman, G. Scalmani, V. Barone, G. A. Petersson, H. Nakatsuji, X. Li, M. Caricato, A. V. Marenich, J. Bloino, B. G. Janesko, R. Gomperts, B. Mennucci, H. P. Hratchian, J. V. Ortiz, A. F. Izmaylov, J. L. Sonnenberg, Williams, F. Ding, F. Lipparini, F. Egidi, J. Goings, B. Peng, A. Petrone, T. Henderson, D. Ranasinghe, V. G. Zakrzewski, J. Gao, N. Rega, G. Zheng, W. Liang, M. Hada, M. Ehara, K. Toyota, R. Fukuda, J. Hasegawa, M. Ishida, T. Nakajima, Y. Honda, O. Kitao, H. Nakai, T. Vreven, K. Throssell, J. A. Montgomery Jr., J. E. Peralta, F. Ogliaro, M. J. Bearpark, J. J. Heyd, E. N. Brothers, K. N. Kudin, V. N. Staroverov, T. A. Keith, R. Kobayashi, J. Normand, K. Raghavachari, A. P. Rendell, J. C. Burant, S. S. Iyengar, J. Tomasi, M. Cossi, J. M. Millam, M. Klene, C. Adamo, R. Cammi, J. W. Ochterski, R. L. Martin, K. Morokuma, O. Farkas, J. B. Foresman and D. J. Fox, *Gaussian 16, Revision C.01*, Gaussian, Inc., Wallin, 2016.

48 A. V Marenich, C. J. Cramer and D. G. Truhlar, *J. Phys. Chem. B*, 2009, **113**, 6378–6396.
49 R. Linder, M. Nispel, T. Häber and K. Kleinermanns, *Chem. Phys. Lett.*, 2005, **409**, 260–264.
50 S. V. Fedorov and L. B. Krivdin, *J. Fluorine Chem.*, 2020, **238**, 109625.
51 G. Saielli, R. Bini and A. Bagno, *RSC Adv.*, 2014, **4**, 41605–41611.
52 M. A. Fox, G. Pattison, G. Sandford and A. S. Batsanov, *J. Fluorine Chem.*, 2013, **155**, 62–71.
53 We attempted to use the calculated GIAO-NMR chemical shifts (ref. 50–52), but obtained inconsistent results. More systematic studies seem to be necessary for the correlation between the observed and calculated chemical shifts for H-bonding ^{19}F.
54 S. S. Lee, S. Park, Y. Hong, J. U. Lee, J. H. Kim, D. Yoon, X. Kong, S. Lee and H. Bin Oh, *Phys. Chem. Chem. Phys.*, 2017, **19**, 14729–14737.
55 H. Choi, Y.-H. Oh, S. Park, S.-S. Lee, H. Bin Oh and S. Lee, *Sci. Rep.*, 2022, **12**, 8169.
56 Y. Oh, H. Bin Oh and S. Lee, *Int. J. Quantum Chem.*, 2024, **124**, e27337.
57 Y.-H. Oh, S. Y. Lee, X. Kong, H. Bin Oh and S. Lee, *ACS omega*, 2024, **9**, 23793–23801.
58 Y.-H. Oh, S. Y. Lee, H. Bin Oh and S. Lee, *Molecules*, 2025, **30**, 1723.